

Microwave-Excited Microplasma Thruster: Design Improvement for Implementation to Satellite

IEPC-2009-190

*Presented at the 31st International Electric Propulsion Conference,
University of Michigan, Ann Arbor, Michigan, USA
September 20–24, 2009*

Takeshi Takahashi*, Shunsuke Kitanishi†, Yoshinori Takao‡, Koji Eriguchi§ and Kouichi Ono¶
Kyoto University, Sakyo-ku, Kyoto, 606-8501, Japan

Abstract: A design improvement of microwave-excited microplasma thruster for implementation to satellites was carried out. We have succeeded to generate plasma and obtain sufficient thrust performance for nanosatellites with the engineering model. However, there are some problems about structure and heat resistance came in sight through experiments and needed to be resolved. With utilizing a numerical simulation previously developed in the design process of this flight prototype, the time and costs for trial and error are highly reduced. The experiments are now underway.

Nomenclature

d	= Diameter of the plasma chamber
f	= Microwave frequency
F_t	= Thrust
I_{sp}	= Specific impulse
l	= Length of the plasma chamber
\dot{m}	= mass flow rate
n_e	= Plasma electron number density
p	= pressure
P_{abs}	= Total absorbed power
T	= Period of the electromagnetic waves
T_h	= Gas temperature
T_w	= Temperature of the chamber wall
u	= Axial flow velocity
u_{eff}	= Effective exhaust velocity
ρ	= density

*Doctoral Student, Department of Aeronautics and Astronautics, t-takahashi@aero.mbox.media.kyoto-u.ac.jp.

†M. C. Student, Department of Aeronautics and Astronautics.

‡Assistant Professor, Department of Aeronautics and Astronautics, takao@kuaero.kyoto-u.ac.jp.

§Associate Professor, Department of Aeronautics and Astronautics, eriguchi@kuero.kyoto-u.ac.jp.

¶Professor, Department of Aeronautics and Astronautics, ono@kuaero.kyoto-u.ac.jp.

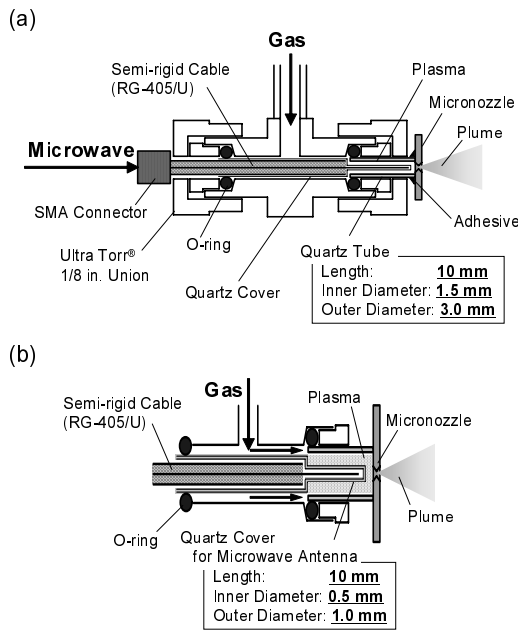


Figure 1. (a) Cross-sectional view of a microplasma thruster, and (b) its radially enlarged view showing the feed of propellant gases.

I. Introduction

IN recent years, the trend of space systems has been focused on miniaturization and simplification of the structure, to reduce the mission costs and increase the launch rates. Missions with numerous small-scale satellites, called “nanosatellites” would bring a significant advantage of reducing the mission risk.¹ Such concept has supported a new approach to develop accurate, reliable, and low-cost micropropulsion systems, particularly for high-accuracy station keeping and attitude control.

In this paper, we report on a microplasma thruster with surface wave-excited plasma (SWP) sources, with emphasis being placed on numerical evaluation of the property of SWP sources by taking into account the spatial distribution of plasma parameters therein. A remarkable feature of SWPs is the electron heating that occurs in a thin skin-depth layer along the plasma-dielectric interfaces; that is, the power absorption in plasmas becomes maximum at interfaces.² This is a great advantage to generate plasmas in a very small space. In effect, the smaller the dimension is, the larger the surface-to-volume ratio is, which leads to a significant diffusion loss to the wall. Another advantage of microwave plasmas is that there is no electrode, and so a serious lifetime problem caused by plasma sputtering is avoided.

Figure 1 shows a cross-sectional view of the previously-developed engineering model, which consists of an azimuthally symmetric surface wave-excited plasma source and a conical micronozzle for exhausting the plasma.³⁻⁷ The microplasma source is composed of a dielectric chamber, 0.75 mm in radius and 10 mm long, and a metal around the chamber.

Microwaves propagate through a coaxial cable which is connected to the left end of the plasma chamber, and then penetrate into the chamber, where the propellant is ionized and heated up by surface waves. The high thermal energy is converted into directional kinetic energy through the nozzle which has a converging and diverging section, to obtain the thrust. We use argon, hydrogen and helium for the propellant.

II. Design Concept of Improved Model

The engineering model has succeeded to generate plasma and obtain sufficient thrust performance for nanosatellites. Stable plasma generation at the microwave power range of 2.0 – 8.0 W with argon, hydrogen, and helium propellants was observed. The thrust F_T and specific impulse I_{sp} were measured to be 0.01 – 1.5 mN and 50 – 700 s, respectively, using argon and hydrogen. This result indicated the possibility of wide-range I_{sp} operation with multiple propellant and only single configuration. For example, high-thrust operation with argon and high- I_{sp} operation with

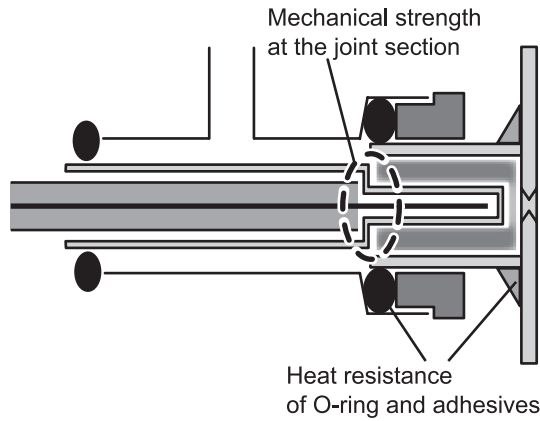


Figure 2. The components in the engineering model, needed to be improved.

hydrogen were suitable for orbit control and attitude control, respectively.

As a next step, we are now designing the improved model for implementation to a satellite. It became clear that the engineering had some problems about structural strength and heat resistance, as shown in Fig. 2. First, the quartz cover for microwave antenna can be often broken by shock and vibration, mainly at the joint section. The O-rings are made of rubber and affected easily by heat, thus the continuous operation time of thruster is limited by this reason. Also, it is predicted that the engineering model is not an optimum configuration for 10-GHz microwave operation (see Sec. III) and redesign is needed. In the design improvement process, we aimed at resolving these structural and heat problems, and making better performance with an aid of presently developed numerical simulation.

III. Numerical Simulation

In this section, the outline of presently developed numerical simulation was described. The calculation area is 1.56 mm in radius and 6.54 – 12.54 mm long, as shown in Fig. 3, containing the plasma chamber and coaxial cable. The calculation cell is $30 \times 30 \mu\text{m}$, and thus the area consists of 52 cells in the radial direction and 218 – 418 cells in the axial direction. In addition, the chamber is made of quartz ($\epsilon_1 = 3.8$), the envelope of the coaxial cable is made of poly-tetrafluoroethylene ($\epsilon_2 = 2.1$), and all metallic parts are treated as perfect conductor.⁷

The numerical model consisted of an electromagnetic module for microwave propagation interacting with plasmas and a fluid module for plasma flows with two (electron and heavy particle) temperatures. The former employed the finite difference time-domain (FDTD) approximation, being applied to the plasma source region, to analyse the microwave power absorbed in the plasma. The latter employed two-temperature fluid equations, being applied to both the source and the nozzle regions, to analyse the plasma and nozzle flow characteristics. Gas-phase reactions were taken into account in the fluid module, along with plasma-wall interactions in a limited space, and the analysis of the nozzle flow finally gave the thrust performance achieved. The working gas of interest in this study was Ar, and the numerical analysis relied on the azimuthally symmetric coordinate system assuming that:

1. The plasma is a two-phase medium consisting of electrons and heavy particles (ions and neutrals), and the temperature of electrons is different from that of heavy particles.
2. The plasma is macroscopically quasi-neutral, or the electron density equals that of ions.
3. The atomic processes in the gas phase are electron-impact excitation/de-excitation and ionization/recombination, taking into account metastable as well as ground-state atoms for neutrals.
4. The charged particles (ions and electrons) diffuse towards the walls according to the ambipolar diffusion.
5. The sheath structures are neglected at the plasma-wall interfaces.
6. The gas/plasma flow is laminar, and the convective velocity is the same for all species (electrons and heavy particles).

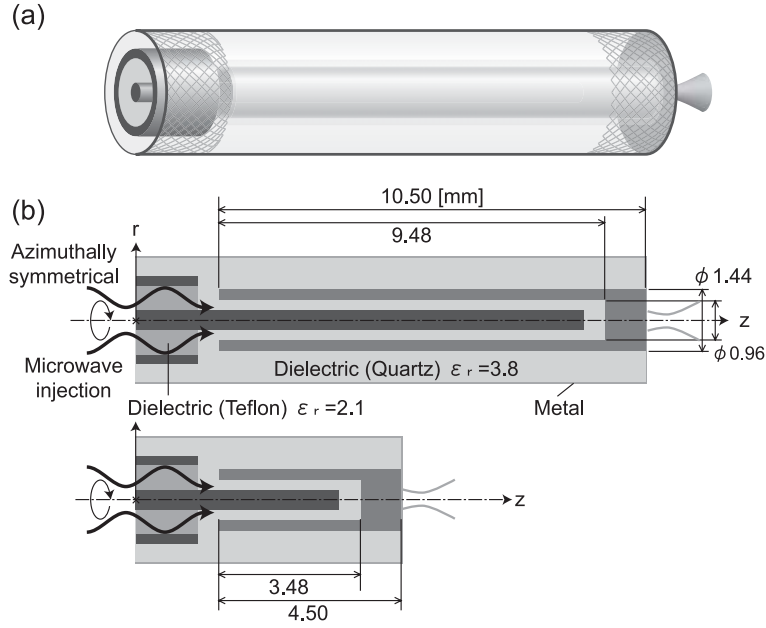


Figure 3. (a) Schematic of the microplasma thruster presently investigated, together with (b) the cross-section. The calculation area is azimuthally symmetric, being 1.56 mm in radius (r direction) and 12.54 / 6.54 mm in axis (z direction).

Table 1. Thrust F_t , specific impulse I_{sp} and power absorption ratio P_{abs}/P_{in} at the conditions same as Fig. 4.

	f [GHz]	l [mm]	F_t [mN]	I_{sp} [s]	P_{abs}/P_{in} [%]
(a)	4.0	10.50	1.18	81.2	83
(b)	10	10.50	1.15	79.4	71
(c)	10	4.50	1.40	95.7	91

7. In the microplasma source, moreover, the microwave energy is absorbed by plasma electrons, which in turn, is transferred to heavy particles through elastic collisions between them.

It should be noted here that this model takes into account the gas/plasma flow self-consistently over the entire region through the microplasma source to the micronozzle (or through subsonic to supersonic).

The simulation was performed with the following conditions for design optimization: mass flow rate of propellant gas $\dot{m} = 0.3 - 2.1$ mg/s (10 - 70 sccm), microwave frequency $f = 4.0 - 10$ GHz, temperature $T_w = 500$ K of the chamber wall, relative permittivity $\epsilon_1 = 3.8$ (quartz) of the chamber, and total input power $P_{abs} = 3.6 - 8.4$ W, length $l = 4.5 - 10.5$ mm, diameter $d = 1.44 - 2.88$ mm of the chamber.

Figure 4 and Table 1 show the results under three conditions as typical examples.

- (a) $f = 4.0$ GHz and $l = 10.50$ mm (the same as present experimental setup, optimum for 4.0-GHz)
- (b) $f = 10$ GHz and $l = 10.50$ mm (higher-frequency microwaves with present setup)
- (c) $f = 10$ GHz and $l = 4.50$ mm (optimum setup for 10-GHz microwaves)

It should be noted that $\dot{m} = 1.5$ mg/s (50 sccm), $P_{in} = 6.0$ W and $d = 1.44$ mm are common among (a)–(c).

As shown in Fig. 4, the propellant gas was heated in front of the nozzle inlet up to ≈ 850 K, and the exhaust gas velocity reached ≈ 800 m/s under the condition (a). This distribution was substantially desirable, and the absorption ratio was 83 % ($P_{abs} \approx 5.0$ W). The thrust F_t and specific impulse I_{sp} was calculated to be 1.18 mN and 81.2 s, respectively, with

$$F_t = \int_0^{r_{ex}} (\rho u^2 + p) r dr \quad (1)$$

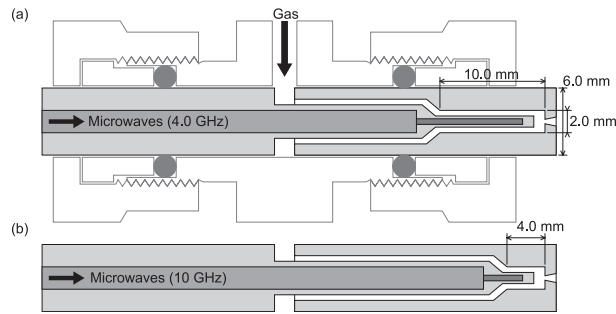


Figure 5. The improved design of micro plasma thruster, in the cross-sectional view. (a) 10.0-mm long plasma chamber for 4.0-GHz operation and (b) 4.0-mm chamber for 10-GHz operation, reflecting the result of numerical analysis.

and

$$I_{sp} = \frac{F_t}{\dot{m}g}. \quad (2)$$

However, when the microwave frequency f was changed to 10 GHz (b), the F_t and I_{sp} went down by 3 % compared with (a). The propellant gas was heated not only in front of the nozzle inlet, but at the side of the antenna cover, because of there were 2 loops of standing waves due to the shorter wavelength. Since the heat loss to the wall was significant, gas heating at the side did not contribute to thrust performance. Also, the power absorption ratio P_{abs}/P_{in} was 71 %, 12 % lower compared with (a).

Then, as shown in Table 1, the thrust performance jumped up by 17% from (a), with shorter plasma chamber (6.0 mm shrunked). The primary reason was considered to be higher power density, because of higher absorption rate and smaller plasma volume. With this configuration, gas heating at the side was not observed and the heavy particle (gas) temperature reached ≈ 1250 K and the exhaust velocity was ≈ 900 m/s.

On the other hand, the equation of specific impulse I_{sp} can be transformed into

$$I_{sp} = \frac{u_{eff}}{g}, \quad (3)$$

using effective exhaust velocity u_{eff} . The flow velocity at the nozzle exit was about 800 – 950 m/s, thus the estimated I_{sp} was 80 – 90 s. This result is sufficiently adequate, taking pressure thrust into consideration.

IV. Improved Design of Micro Plasma Thruster

Figure 5 shows the cross-sectional view of the improved model. First, the microplasma chamber and the micronozzle are unified into single component, made from 6.0-mm-diameter quartz block. The joint section is also thickened to increase the mechanical strength against shock and vibration. From the result of numerical analysis mentioned in Sec. III, the length of plasma chamber is (a) 10.0 mm and (b) 4.0 mm, for operation with 4.0-GHz and 10-GHz microwaves, respectively. Swagelok Ultra-Torr® union is used for mounting the thruster, since it has sufficient vacuum sealing and ease of adjustment. Also, the distance between the O-ring and the plasma chamber was extended compared with the engineering model, thus a longer continuous operation is enabled. It is noted that long antenna cover and coaxial cable are mainly for reasons of experimental setup, and they are not needed in implementation to the nanosatellite. Figure 6 shows a photographic image of this improved model, and the components are fabricated by micro-machining of quartz. We are now working with the experiments.

V. Conclusions

Electrothermal-type microplasma thruster has succeeded to generate plasma and obtain sufficient thrust performance for nanosatellites with the prototype model. The results indicated the possibility of wide-range I_{sp} operation with multiple propellant and only single configuration. For example, high-thrust operation with argon and high- I_{sp} operation with hydrogen were suitable for orbit control and attitude control, respectively. A design improvement for implementation to satellites was carried out, in order to resolve some problems about structure and heat resistance

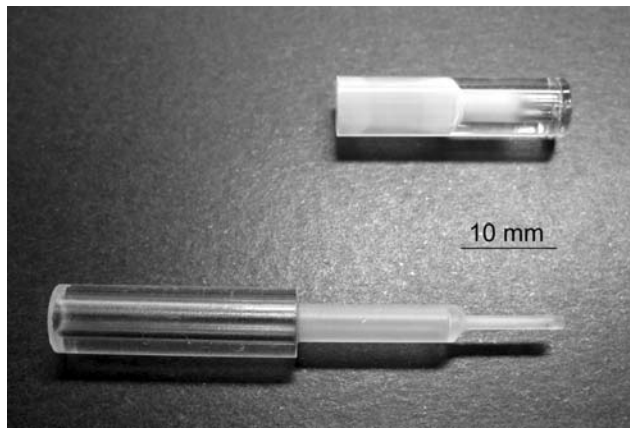


Figure 6. The photographic image of micro plasma thruster.

came in sight through experiments. With utilizing a numerical simulation previously developed in the design process, the time and costs for trial and error are highly reduced. The experiments are now underway.

References

- ¹Mueller, J., "Thruster Options for Microspacecraft: A Review and Evaluation of Existing Hardware and Emerging Technologies", *Proceedings of 33rd AIAA/ASME/SAE/ASEE Joint Propulsion Conference*, 1997, Article No. AIAA 97-3058.
- ²Ganachev, I., and Sugai, H., "Advanced large-area microwave plasmas for materials processing", *Surface & Coatings Technol.*, Vol. 174-175, 2003, pp. 15–20.
- ³Takao, Y. and Ono, K., "A miniature electrothermal thruster using microwave-excited plasmas: a numerical design consideration", *Plasma Sources Sci. Technol.*, Vol. 15, 2006, pp. 211–227.
- ⁴Takao, Y., Ono, K., Takahashi, K., and Eriguchi, K., "Plasma Diagnostics and Thrust Performance Analysis of a Microwave-Excited Microplasma Thruster", *Jpn. J. Appl. Phys.*, Vol. 45, 2006, pp. 8235–8240.
- ⁵Takao, Y., Eriguchi, K. and Ono, K., "A miniature electrothermal thruster using microwave-excited microplasmas: Thrust measurement and its comparison with numerical analysis", *J. Appl. Phys.*, Vol. 101, 2007, Article No. 123307.
- ⁶Takahashi, T., Takao, Y., Eriguchi, K. and Ono, K., "Microwave-excited microplasma thruster: a numerical and experimental study of the plasma generation and micronozzle flow", *J. Phys. D: Appl. Phys.*, Vol. 41, 2008, Article No. 194005.
- ⁷Takahashi, T., Takao, Y., Eriguchi, K. and Ono, K., "Numerical and experimental study of microwave-excited microplasma and micronozzle flow for a microplasma thruster", *Phys. Plasmas*, Vol. 16, 2009, Article No. 083505.